VI.2. FISCHER-TROPSCH SYNTHESIS: MÖSSBAUER STUDIES OF PRETREATED ULTRAFINE IRON OXIDE CATALYSTS (Chen-Shi Huang, Bhaswati Ganguly, Gerald P. Huffman, Frank E. Huggins, and Burtron H. Davis).

VI.2.1. ABSTRACT

Mössbauer spectroscopy indicates that a 24 hour pretreatment in CO at 260°C and 8 atm. in a tetralin solvent almost completely converts ultrafine iron oxide (about 3 nm) to iron carbide. However, pretreatment in hydrogen under the same conditions resulted in reduction of about 33% of the iron to metallic Fe; the remainder was Fe_3O_4. Exposure of the CO pretreated catalyst to a 1:1 H_2/CO synthesis gas resulted in the gradual reoxidation of the carbides to Fe_3O_4. During the first 2 hours of exposure of the H_2 pretreated sample to synthesis gas, the metallic Fe was converted to iron carbides. Further exposure of the H_2 pretreatment sample to synthesis gas did not result in a composition change of the catalyst. Therefore, it is concluded that iron carbides with different oxidation characteristics were formed in these two cases.

VI.2.2. INTRODUCTION

Pretreatment has a great impact on the compounds present in iron catalysts and on the Fischer-Tropsch (FT) synthesis activity and selectivity. For a catalyst pretreated in hydrogen at 300°C or above, iron may initially be present in the metallic state. However, it converts rapidly to carbide phases or oxides when exposed to syngas under reaction conditions (VI.2.1-VI.2.6). An oxide catalyst that is pretreated in CO or directly exposed to syngas may be converted from Fe_2O_3 to low valence oxides or carbides (VI.2.5,VI.2.7,VI.2.8). In these cases, the composition of the iron

phases changes with pretreatment and reaction time (VI.2.9-VI.2.11). It has been reported that pretreatment in CO results in a better catalyst than one pretreated in hydrogen (VI.2.5,VI.2.10,VI.2.11). Many studies have aimed at defining the active iron phase by correlating the structure of the catalyst to FT synthesis activity (VI.2.1,VI.2.2,VI.2.5,VI.2.6,VI.2.9,VI.2.12-VI.2.15). However, there is no clear consensus as to which phase provides the superior activity (VI.2.10,VI.2.11).

A recent study focused on the effect of pretreatment on the structure, catalytic activity and selectivity of a high surface area Fe_2O_3 catalyst in a continuously stirred tank reactor (CSTR) (VI.2.16). Catalyst samples were withdrawn periodically from the reactor and characterized by X-ray diffraction (XRD) and transmission electron microscopy (TEM). It was of interest to utilize Mössbauer to characterize further the chemical states of iron in a series of catalysts during similar pretreatment and synthesis conditions.

VI.2.3. EXPERIMENTAL

VI.2.3.a. Catalyst Activation and Syngas Reaction

A process scheme described earlier (VI.2.16) that employed a 300 mL CSTR was used for the present study. A slurry of 5.0g of ultrafine Fe_2O_3 (United Technologies, surface area 270 m^2/g) in 380 cc octacosane (Fisher, 99%) was charged into the CSTR. Pretreatment gas was introduced and the reactor was pressurized to 105 psig (8 atm absolute). The temperature of the reactor was then increased from ambient to 260°C at a rate of 1.5°C/min with a gas flow rate of 2.57 L/g-Fe/h (or 5.57 L/g-Fe/h for a H_2/CO = 1.03 mixture) and a stirring rate of 1200 rpm. The reactor was then held at 260°C for 24 hrs. After activation, syngas (H_2/CO= 1.03)

was introduced to the reactor at a flow rate of 2.57 L/g-Fe/h. CO and H_2 conversions and gas product selectivities were obtained by analysis of the exit gas using a Carle gas analyzer. During the activation process and the syngas reaction period, a small amount of catalyst was withdrawn from the reactor at several designated times for characterization.

VI.2.3.b. Mössbauer Spectroscopy

The Mössbauer experiments were carried using a constant acceleration spectrometer described in more detail elsewhere (VI.2.17-VI.2.20). The radioactive source consisted of 50-100 mCi of ^{57}Co in a Pd matrix. The samples were in powder form and were loaded into Plexiglass compression holders presenting a thin aspect to the gamma ray beam. All spectra were analyzed by a least-squares fitting procedure which models the spectra with a series of Lorentzian peaks. The percentages of the total sample iron contained in each iron-bearing phase identified are determined from the relevant peak areas by procedures discussed in earlier papers (VI.2.17,VI.2.19).

VI.2.4. RESULTS

The first series to be considered is the material treated in hydrogen for 24 hours. After 24 hours of reduction at 260°C, the Mössbauer spectrum (Figure VI.2.1) showed that the catalyst was a mixture of metallic iron (36%) and magnetite (64% of the iron; 32% a-site and 32% B-site) (Table VI.2.1). After the catalyst was exposed for 2 hours to the syngas mixture (CO/H_2 = 1.03), the Mössbauer spectrum (Figure VI.2.2) showed that the magnetite portion of the catalyst was essentially unchanged; however, the metallic iron had been converted to a mixture of $Fe_{2.2}C$ (24% of the iron, 2% in superparamagnetic (spm) form) and Fe_3C (12% of the iron). Mössbauer

spectra taken after 11 hours (Figure VI.2.3) and 24 hours exposure to the syngas mixture were essentially identical to that obtained after 2 hours. The iron phase percentage observed after 11 and 24 hours were identical, within the accuracy of the measurement: magnetite - 63%, Fe_3C - 10%; $Fe_{2.2}C$ - 27% (3-5% spm). It should be noted that the accuracy of the iron phase percentages is approximately $\pm$ 2-3%. Therefore, the identification of minor phases containing less than about 5% of the total iron is considered to be somewhat uncertain. However, the presence of such minor phases does not materially affect the conclusions of this research.

The percentages of iron contained in the observed phases for the samples exposed to syngas following 24 hours reduction at 260°C in hydrogen are shown as a function of exposure time in Figure VI.2.4. It is evident that the only change during the syngas treatment is the transformation of the metallic iron formed during the hydrogen reduction to the iron carbides. There is essentially no change in the amount of Fe_3O_4 during the 24 hour exposure to syngas.

The next series of catalysts that were characterized had been exposed to CO for 24 hours at 260°C and then for increasing time in a syngas mixture. The sample, after 24 hours exposure to CO, is present only in carbide forms (Figure VI.2.5). Only 4% of the sample iron is present as an unidentified ferrous iron oxide. The peaks corresponding to 220 and 180 kG are due to χ-Fe_5C_2, and this accounts for 63% of the total iron. It is not possible to identify the phase of the iron carbide that produces the absorption at 104 kG that accounts for 33% of the total iron. It may represent a surface or vacancy perturbed component of the Fe_5C_2 phase.

After 2 hours exposure to the syngas, the Mössbauer spectrum (Figure VI.2.6) has undergone changes from the one obtained following 24 hours in CO. Because of the complexity of the spectrum and the poor signal/noise ratio, a satisfactory fit to the data could not be obtained. Based upon the incomplete fit, it is estimated that about 33% of the iron is present as magnetite and the remainder as a complex mixture of iron carbides.

Exposure to the syngas for 10 hours resulted in a further change in the sample and the Mössbauer spectrum shown in Figure VI.2.7. During this period, further oxidation of the carbides occurred so that 57% of the iron is present as magnetite (20% A-site and 37% B-site). The iron carbides were mostly the χ-Fe_5C_2 phase.

Exposure of the sample to syngas for 48 hours resulted in additional oxidation of the iron carbide (Figure VI.2.8). Magnetite (37% A-site and 53% B-site) now constituted 90% of the iron. The iron carbide may be χ-Fe_5C_2 or ϵ'-$Fe_{2.2}C$; it is not possible to make a positive identification from the spectrum.

After exposure to syngas for 100 hours, the catalyst was completely oxidized so that only magnetite peaks are observed in the spectrum (Figure VI.2.9; 43% A-site and 57% B-site).

The changes of the iron compounds over the 100 hour period of exposure to syngas are shown in Figure VI.2.10. It is apparent that the carbide formed during the pretreatment in CO is not stable under the conditions existing during the period of exposure to the synthesis gas. Reoxidation continues throughout so that only magnetite was observed after 100 hours of exposure to the syngas.

The conversion data for these two catalyst pretreatment series are shown in Tables VI.2.2 and VI.2.3. For the hydrogen pretreated sample, there is a decrease in the CO conversion from 2 to 10 hours on stream and after this time the CO conversion does not change; the hydrogen conversion remains constant throughout the run (Figure VI.2.11). For the CO pretreated sample, both CO and hydrogen conversion nearly doubles from 2 to 10 hours on syngas; this is followed by a marked decline in conversion from 10 to 24 hours on stream (Figure VI.2.11). From 24 to 120 hours on syngas, both the CO and hydrogen conversion decline by nearly 50%. Thus, even though it was not possible to control precisely the amount of catalyst that was withdrawn during the course of the reaction, it is clear that the two pretreatments lead to different activity patterns following exposure to syngas.

The CO pretreated catalyst produces a higher fraction of methane, C_2 and C_3 hydrocarbons during syngas conversion even during the period when the conversions are similar. The C_4^+ fraction has been calculated from the difference in CO feed rate and the gaseous products (CO_2, CH_4, C_2 and C_3). For the course of the run the C_4^+ fraction is higher for the hydrogen pretreated sample (Figure VI.2.12).

VI.2.5. DISCUSSION

There is general agreement between the Mössbauer data of this study and the characterization results reported earlier for two series of samples with the same pretreatments (VI.2.16). XRD studies conducted earlier clearly indicated that CO is a better reducing agent than H_2. These results are consistent with a static TG/DTA study which showed that CO is better than H_2 for the reduction of α-Fe_2O_3 (VI.2.21). The incomplete transformation of Fe_2O_3 to iron carbide after 24 hours of activation in

The present Mössbauer data yield somewhat different conclusions. In particular, it is found that the catalyst is completely reduced to carbide during CO activation and that the carbide formed is predominantly Fe_5C_2 (chi-carbide). This carbide is converted to Fe_3O_4 during syngas conversion as shown in Figure VI.2.10. Hydrogen activation, however, yields a catalyst in which 36% of the iron is present as iron metal and 64% as magnetite. During syngas conversion, the iron metal is quickly converted to a carbide mixture that appears to be quite stable and shows no conversion to magnetite after 24 hours of treatment, as shown in Figure VI.2.4. The carbide formed from iron metal during syngas treatment is a mixture consisting of approximately 1/3 Fe_3C (cementite) and 2/3 $Fe_{2.2}C$; these carbides apparently resist oxidation much better during syngas treatment than does Fe_5C_2.

Carbide phases were often observed in earlier studies of Fe catalysts (VI.2.5,VI.2.8). However, the catalysts in those studies are low surface area materials or contain alkali promoters. An outer layer of large particles of catalysts may retard oxidation of carbide or metallic phase. The alkali promoter which has been reported to accelerate carburization is also expected to stabilize the carbidic phases. Thus in the present study, the use of higher surface area Fe_2O_3 and the lack of alkali promoter in the catalyst may be the reason for the observation of only Fe_3O_4 by XRD in the catalysts after 10 or more hours of syngas conversion.

The XRD patterns in the earlier study (VI.2.16) indicate that Fe_3O_4 is the only crystalline phase present for the catalyst at the point of maximum activity, and this does not depend upon the activation gases. Huang et al. (VI.2.16) took this to imply that Fe_3O_4 is the active phase, or that the active phase can not be detected by XRD.

CO, as indicated by our XRD data, is consistent with a Mössbauer spectroscopic study that showed the presence of magnetite and Fe_5C_2 in an amorphous Fe_2O_3 after 24 hours of activation in CO at 270°C (VI.2.22). However, Zarochak and McDonald have reported a complete transformation of Fe in a Fe-K-Cu (65:0.29:0.6) catalyst to carbidic iron at 280°C and under 200 psig CO during 24 hours in a slurry phase autoclave (VI.2.10). The presence of K, which has been reported to accelerate carburization (VI.2.23,VI.2.24), as well as the higher temperature (280 vs. 260°C) and pressure (200 vs. 105 psig) in their study, were offered as possible explanations for the difference between their results and our earlier results. However, our Mössbauer data for the ultrafine unpromoted iron oxide catalyst used in this study indicate that essentially all of the oxide was converted to the carbide by a 24 hour treatment with CO at 260°C and 7 atm. Considering the past and current data, it appears that the iron is mostly present in a carbide form following CO pretreatment; this appears to be true whether or not a K promoter is present.

The observation that only 36% of the iron is converted to a metallic form after 24 hours activation in H_2 at 260°C is surprising, but this has also been reported (VI.2.22). It is possible that the condenser in the reactor set-up (Figure VI.2.1) which was used to trap tetralin vapor may also condense water vapor during the course of reaction; this water may reoxidize metallic Fe to Fe_3O_4.

After 10 h of syngas conversion, the catalysts activated in hydrogen and CO showed only Fe_3O_4 by XRD. This has been reported for catalysts which showed mainly iron carbide or α-Fe phase after activation (VI.2.10,VI.2.25), and has been attributed to the presence of water vapor, particularly at high conversion.

The Mössbauer data indicate that this conclusion must be modified, at least for the CO pretreated material where carbide as well as oxide is present (Figures VI.2.10 and VI.2.11). However, the fact that, after 2 hours in syngas, Fe_2O_3 already has been completely transformed into Fe_3O_4 and that this material shows only minimum activity while a Fe_3O_4 phase that was observed for the catalyst activated in H_2 for 24 h showed a much higher activity, indicates that bulk Fe_3O_4 is not likely to be the active phase for CO hydrogenation. Furthermore, at maximum activity, the particle size of Fe_3O_4 for the catalyst activated in CO was 74% of that for the catalyst activated in hydrogen. The maximum CO conversion for the CO activated catalyst, however, was 2 times that of the catalyst activated in hydrogen. Therefore, the presence of an active surface or bulk phase supported on the surface of Fe_3O_4 is likely.

Magnetite is a member of the spinel group which has a unit cell of 32 close-packed oxygen atoms in which 8 tetrahedral (A) and 16 octahedral (B) sites can be occupied by the cations [(VI.2.26). In normal spinels, 8 divalent cations per unit cell occupy the A sites and 16 cations occupy the B sites. Inverse spinels have 8 divalent cations in the B sites with trivalent cations in the remaining 8 B and the A sites. In the room temperature Mössbauer spectrum of magnetite, the A to B site iron ratio is typically 1:1.8 - 1.9 [(VI.2.27); this is close to the theoretical value of 1:2 for the ideal spinel structure. In addition, an A:B ratio considerably less than 2 measured by Mössbauer spectroscopy may indicate the presence of B site vacancies and compositions intermediate between Fe_3O_4 and γ-Fe_2O_3 (which also has the spinel structure).

Norval and Phillips (VI.2.28) reported the A to B site ratio for the oxidized form of several commercial iron ammonia synthesis catalysts which contained small amounts of aluminum, silicon, potassium and/or potassium promoters. The reported values of A to B ranged from 1:0.9 to 1:1.3. The ratio for the ICI 35-4 catalyst (containing the wt.% indicated Al, 1.4; Si, 0.6; K, 1.7; and Ca, 1.9) had a ratio of 1:0.9, which was in excellent agreement with the ratios of 1:0.9 -1.0 reported by others (VI.2.29,VI.2.30).

Thus, while several investigators have obtained an A to B ratio that was near 1:1, they utilized promoted iron oxide materials so that it was reasonable to explain the low ratio by a preferential substitution of the B sites by the promoter. However, for the oxide present after either H_2 or CO pretreatment, and at all times during exposure to syngas, the A to B site ratio is very close to 1:1; these values are summarized in Table VI.2.4. The ratio for the material following reduction for 24 hours in hydrogen is 1:1; this ratio increases only marginally, if at all, during 24 hours exposure to the synthesis gas. It appears that the magnetite formed by oxidation, during 100 hours of exposure to the synthesis gas, of the iron carbides formed during the CO pretreatment, has an A to B site ratio that is greater than that of the hydrogen pretreated sample. It therefore appears that the magnetite phases present in the materials pretreated with H_2 and CO are not the same following the pretreatment and synthesis.

The attainment of a similar selectivity independent of the initial pretreatment in the earlier study (VI.2.16) suggested the same, or at least similar active phase(s). It has been proposed that, under reaction conditions, a number of compounds coexist on the surface of an iron catalyst: iron oxides, iron carbides and metallic iron

(VI.2.31). Iron carbides have been proposed as the active phase (VI.2.2,VI.2.9), and that the fraction of iron carbides on the catalyst surface determines the activity (VI.2.9). Others, however, have proposed that metallic iron (VI.2.14,VI.2.15), or iron oxides (VI.2.32-VI.2.34) are the active phases. In the present study, the nature of the active sites was not determined. Nevertheless, the present study suggests that a common, or at least similar, active phase can be obtained after a period of syngas conversion. Furthermore, the amount of iron carbide, if it is the active form of iron, is too small in these catalysts to be easily detected in the Mössbauer spectra.

On iron catalysts, the FT conversion is inevitably accompanied by an internal WGS reaction. The Fe_3O_4 phase is claimed to be active for the WGS reaction (VI.2.35, VI.2.36). There is evidence that the regnearative mechanism is operative in catalyzing the WGS reaction over magnetite. The local partial pressure of H_2O could be a factor determining the relative amounts of carbide and magnetite phases.

VI.2.6. ACKNOWLEDGMENT

The authors acknowledge the financial support of this work by the Department of Energy contract No. DE-AC22-91PC90056 and by the Commonwealth of Kentucky.

VI.2.7. REFERENCES

VI.2.1. Amelse, J. A.; Schwartz, L. H.; and Butt, J. B. *J. Catal.*, **72**, 95 (1981).

VI.2.2. Raupp, G. B. and Delgass, W. N. *J. Catal.*, **58**, 348 (1979).

VI.2.3. Shen, W. M.; Dumesic, J. A.; and Hill, C. G. *Rev. Sci. Instrum.*, **52**, 858 (1981).

VI.2.4. Dry, M. E., "Catalysis-Science and Technology" (Eds J. R. Anderson and M. Boudart), Vol 1, 160-255 (1981).

VI.2.5. Anderson, R. B. in "Catalysis" edited by P. H. Emmett, Van Nostrand-Reinhold, New York, 1956, Vol IV, pp 29-255.

VI.2.6. Satterfield, C. N.; Hanlon, R. T.; Tung, S. E.; Zou, Z.; and Papaefthymiou, G. C. *Ind. Eng. Chem. Prod. Res. Dev.*, **25**, 401-414 (1986).

VI.2.7. Pennline, H. W.; Zarochak, M. F.; Stencel, J. M.; and Diehl, J. R. *Ind. Eng. Chem. Res.*,. **26**, 595-601 (1987).

VI.2.8. Dictor, R. A. and Bell, A. T. *J. Catal.*, **97**, 121-136 (1986).

VI.2.9. Niemantsverdriet, J. W. and Van Der Kraan, A. M. *J. Catal.*, **72**, 385-388 (1981).

VI.2.10. Zarochak, M. F. and McDonald, M. A. *Proceed. Indirect Liquefaction Contractor Meeting*, Dec 1986, Pittsburgh, pp 58-82.

VI.2.11. Bukur, D. B.; Lang, X.; Rossin, J. A.; Zimmerman, W. H.; Rosynek, M. P.; Yeh, E. B.; and Li, C. *Ind. Eng. Chem. Res.*, **28**, 1130-1140 (1989).

VI.2.12. Matsumoto, H. and Bennett, C. O. *J. Catal.*, **52**, 331 (1978).

VI.2.13. Dwyer, D. J. and Hardenbergh, J. H. *J. Catal.*, **87**, 66-76 (1984).

VI.2.14. Dwyer, D. J. and Somorjai, G. A. *J. Catal.*, **52**, 291 (1978).

VI.2.15. Kerbs, H. J.; Bonzel, H. P.; and Gafner, G. *Surface. Sci.*, **88**, 269 (1979).

VI.2.16. Huang, C. S.; Xu, L.; and Davis, B. H. *Fuel Sci. & Technol. Int.*, **1992**, in press.

VI.2.17. Huffman; G.P.; Huggins, F.E. *Fuel*, **1978**, *47*, 592-604.

VI.2.18. Huffman, G.P.; Huggins, F.E. *ACS Advances in Chemistry Series, 194,* "Mossbauer Spectroscopy and Its Chemical Applications", Eds., Stevens, J.G.; Shenoy, G.K.; Amer. Chem Soc., **1981**, 265-301.

VI.2.19. Huggins, F.E.; Huffman, G.P. *Analytical Methods for Coal and Coal Products, Vol.III*, Ed., Karr, Jr.,C.; Academic Press, **1979**, pp. 372-423.

VI.2.20 Huffman, G.P. *Chemtech*, **1980**, *10*, 504-511.

VI.2.21. Richard, M. A.; Soled, S. L.; Fiato, R. A.; and Derites, B. A. *Mat. Res. Bull.*, **18**, pp 829-833 (1983).

VI.2.22. Berry, F. J. and Smith, M. R. *J. Chem. Soc. Faraday Trans. I*, **85(2)**, 467-477 (1989).

VI.2.23. Pichler, H. and Merkel, H. "US Bureau of Mines Tech. Paper", 718 (1949).

VI.2.24. Vogler, G. L.; Jiang, X.-Z.; Dumesic, J. A.; and Madon, R. J. *J. Catal.*, **89**, 116 (1984).

VI.2.25. Jellinek, M. H. and Frankuchen, I. in "Advance in Catalysis", Vol 1, Academic Press, 279, (1948).

VI.2.26. Murad, E. and Johnson,J. H., in "Mössbauer Spectroscopy Applied to Inorganic Chemistry", Plenum Press, New York, NY, 1987, Vol. 2, pp 512-13.

VI.2.27. Topsφe, H. and Mφrup, *Proc. Int. Conf. Mössbauer Spec.*, **1**, 321 (1975).

VI.2.28. Norval, G. W. and Phillips, M. J.; *J. Phys. Chem.*, **90**, 4743 (1986).

VI.2.29. Yoshioka, Y.; Koezuka, J.; and Toyoshima, I.; *J. Catal.*, **14**, 281 (1969).

VI.2.30. Peev, T., *Monats. Chem.*, **107**, 1259 (1976).

VI.2.31. Niemantsverdriet, J. W.; Flipse, C. F. J.; Van Der Kraan, A. M.; and Van Loef, J. J. *Appl. Surf. Sci.*, **10**, 302-313 (1982).

VI.2.32. Reymond, J. P.; Meriadeau, P.; and Teichner, S. J. *J. Catal.*, **75**, 39-48 (1982).

VI.2.33. Blanchard, F. B.; Raymond, J. P.; Pommier, B.; and Teichner, S. J. *J. Mol. Catal.*, **17**, 171-181 (1982).

VI.2.34. Hofer, L. J. E., in "Catalysis" edited by P. H. Emmett, Van Nostrand-Reinhold, New York, 1956, Vol IV, pp 373-441.

VI.2.35. Newsome, D. S. *Catal. Rev. - Sci. Eng.*, **21**, 275 (1980).

VI.2.36. Rethwisch, D. G. and Dumesic, J. A. *Appl. Catal.*, **21**, 97 (1986).

Table VI.2.1

The Compositions of the Ultrafine Iron Catalysts Pretreated in CO or H_2 and then Exposed at 260°C to Synthesis Gas ($CO:H_2$ =1) at 7 atm.

Hydrogen Pretreatment

Time in Syngas Hrs.	Fe	$Fe_{2.2}C$	Fe_5C_2	Fe_3C	Other Phases	Magnetite	
						A-Site	B-Site
0	36					32	32
2		22		12	2[a]	32	33
11		24		10	2[a]	29	34
24		23		10	5[a]	30	33

CO Pretreatment

0			64		33[b]; 4[a]		
2			66[c]			30[c]	
10			22		21[b]	20	37
48			8		2[a]	37	53
100						43	57

a. Minor, inconclusively identified, phases.
b. Iron carbide, unassigned; possibly a component of Fe_5C_2.
c. Based on incomplete fit, mixture of carbides and ca. 30% magnetite.
d. Ferric oxide.

Table VI.2.2

Syngas Conversion Data for the CO Pretreated Catalyst[a]

Run Time, Hr.	2	10	24	40	120
CO conv., %	34.2	88.6	48.2	35.3	23.3
H_2 conv., %	46.9	68.9	48.8	46.2	30.0
H_2/CO usage	1.61	0.93	1.22	1.37	1.54
CO_2 select., %	28.8	38.2	37.6	30.9	28.1
CH_4, %	8.6	4.4	4.6	5.4	8.1
C_2, %	3.1	2.4	2.6	2.9	4.0
C_3, %	3.0	3.3	3.7	3.2	3.6
$C_2^=/C_2$ ratio	0.69	0.32	0.54	0.41	0.38
$C_3^=/C_4$ ratio	3.09	1.96	2.50	2.95	2.80
C_4^+, %	56.5	51.7	51.5	57.6	56.2

[a] Note: % CO_2 + % CH_4 + % C_2 + % C_3 + % C_4^+ = 100.

Table VI.2.3

Synthesis Gas Conversion Data for the H_2 Pretreated Catalyst[a]

Run Time, Hr.	2	10	24	40	120
CO conv., %	72.6	46.4	45.7	45.8	41.4
H_2 conv., %	53.5	43.7	42.6	41.7	37.4
H_2/CO usage	0.88	1.13	1.12	1.09	1.08
CO_2 select., %	17.6	22.7	24.2	25.7	25.8
CH_4, %	3.5	3.5	3.5	4.3	4.4
C_2, %	1.5	1.7	1.8	1.9	1.8
C_3, %	1.7	2.1	2.3	2.1	2.1
$C_2^=/C_2$ ratio	0.19	0.44	0.29	0.35	0.34
$C_3^=/C_4$ ratio	0.96	2.28	2.06	2.09	1.88
C_4^+, %	75.7	70.0	68.2	66.0	65.9

[a] Note: % CO_2 + % C_1 + % C_2 + % C_3 + % C_4^+ = 100.

Table VI.2.4

The A to B Site Occupancy Ratio for the Magnetite Phase in the Catalysts

Pretreatment	Exposure to Synthesis Gas, hrs.	A to B Ratio
H_2	0	1:1
H_2	2	1:1
H_2	11	1:1.2
H_2	24	1:1.1
CO	10	1:1.2
CO	48	1:1.4
CO	100	1:1.3

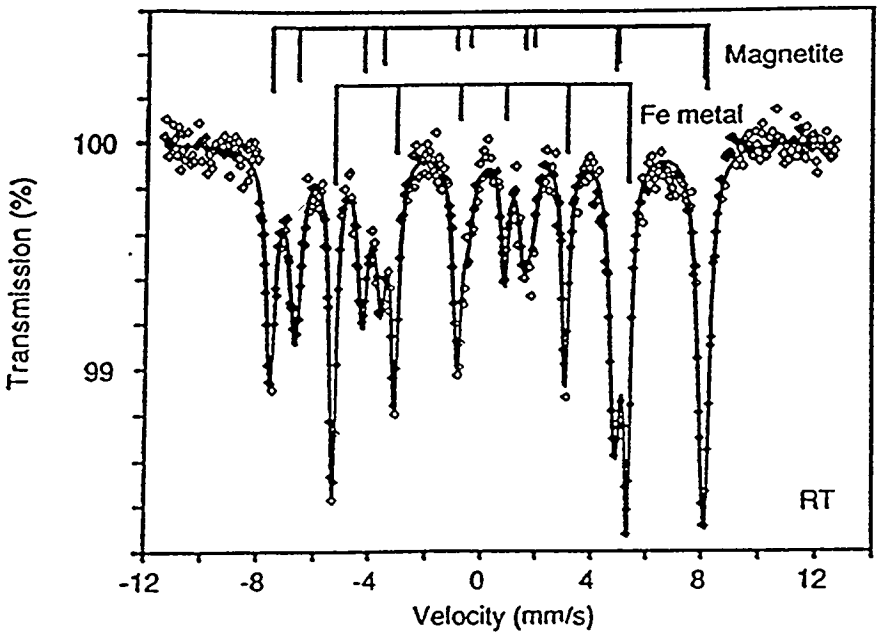

Figure VI.2.1. Mössbauer spectrum of the ultrafine iron oxide following 24 hours in flowing hydrogen at 260°C for 24 hours.

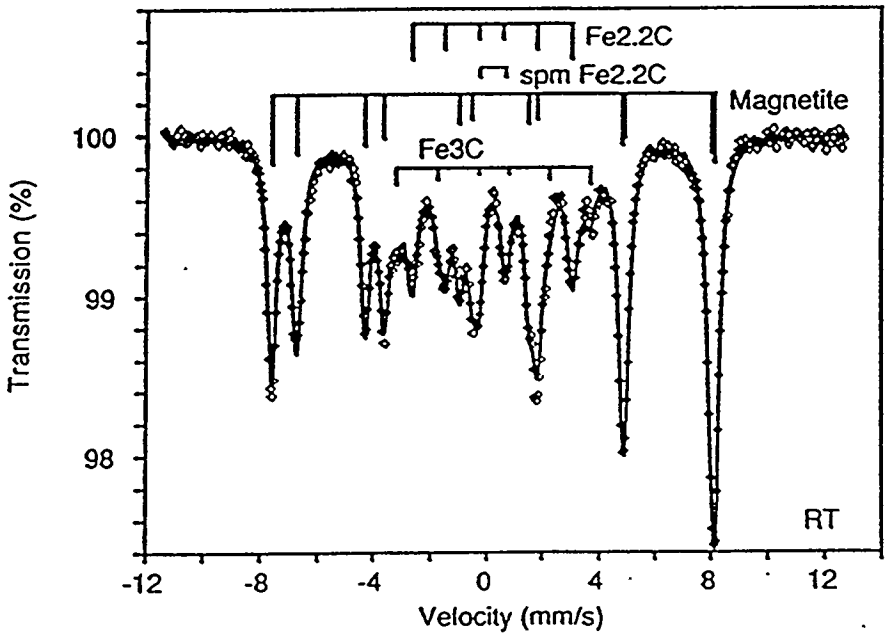

Figure VI.2.2. Mössbauer spectrum of the material from Figure 1 following 2 hours in synthesis gas (CO/H_2 = 1.03) at 260°C.

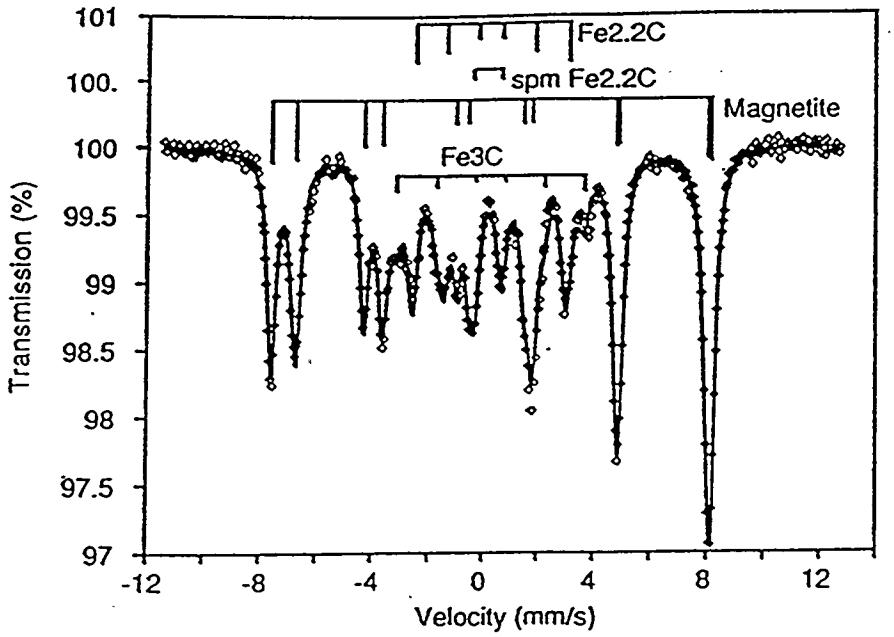

Figure VI.2.3. Mössbauer spectrum of the sample in Figure 2 following 11 hours exposure to syngas.

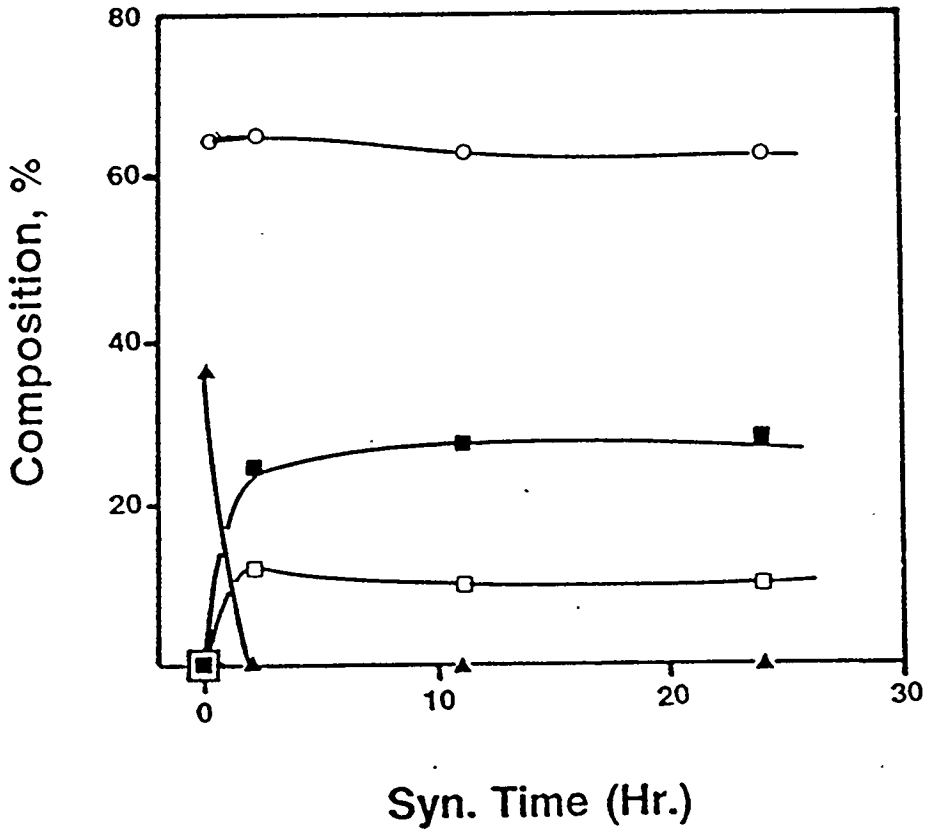

Figure VI.2.4. The change with exposure time in syngas of the iron chemical state following 24 hours of pretreatment in hydrogen (Fe, ▲; $Fe_{2.2}C$, ■; Fe_3C, □; Fe_3O_4, ○).

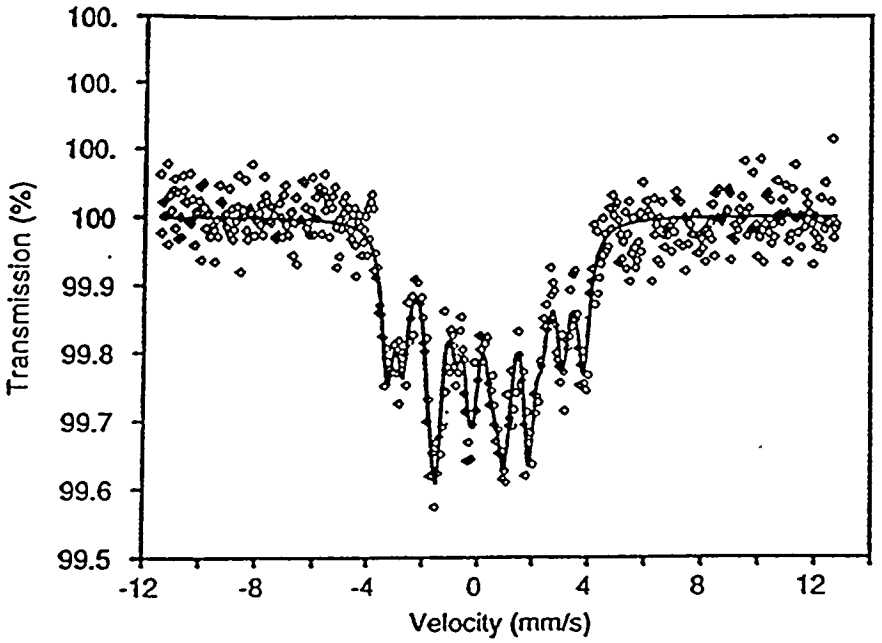

Figure VI.2.5. Mössbauer spectrum of the iron oxide following 24 hours pretreatment in CO at 260°C.

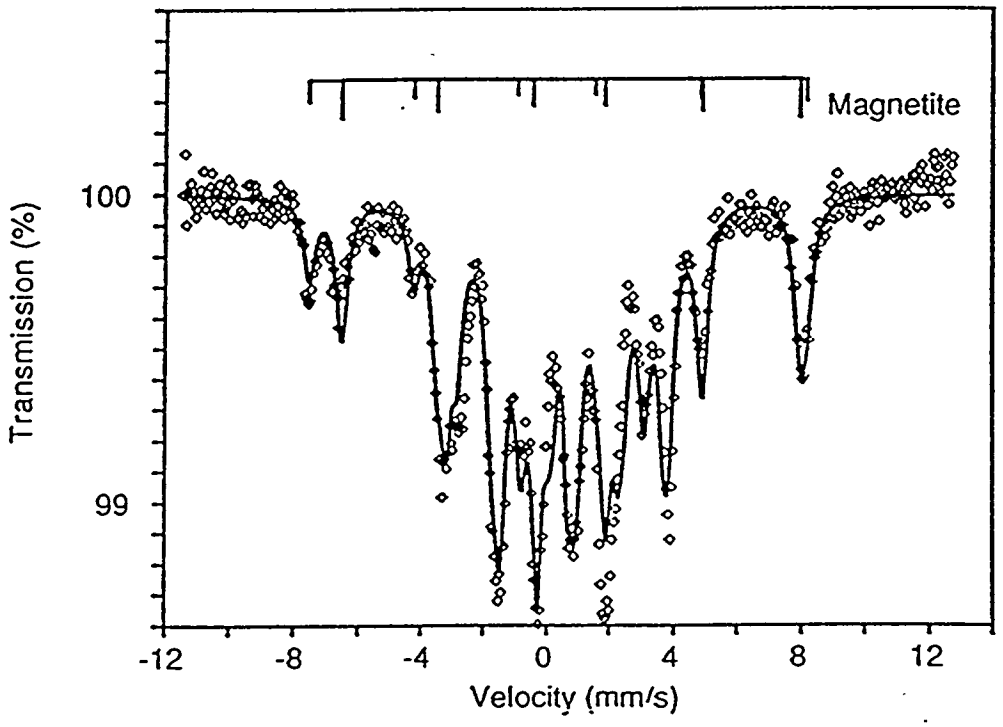

Figure VI.2.6. Mössbauer spectrum of the sample of Figure 5 following 2 hours of exposure to synthesis gas (CO/H_2 = 1.03) at 260°C.

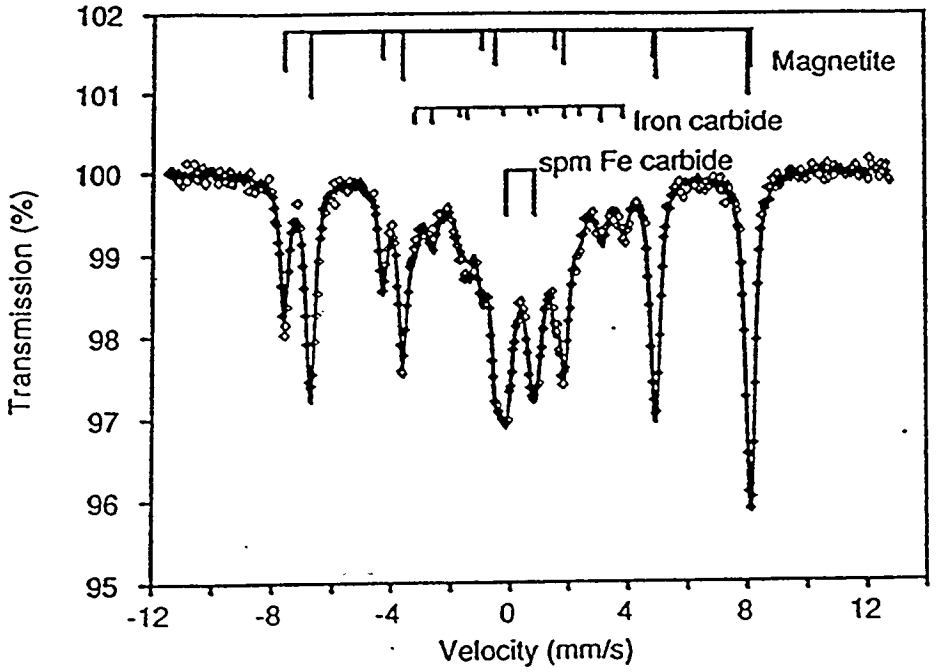

Figure VI.2.7. Mössbauer spectrum of the sample of Figure 5 following 10 hours exposure to syngas.

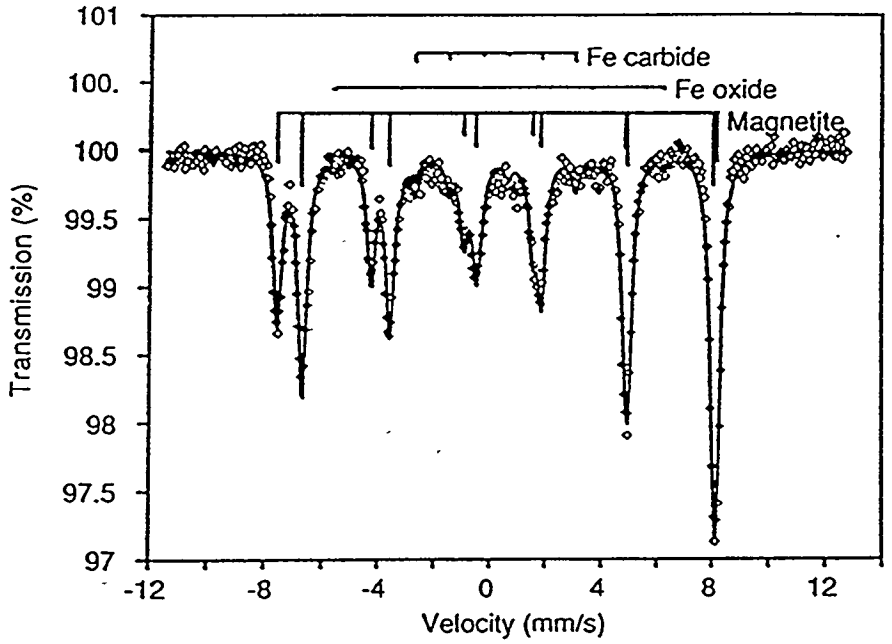

Figure VI.2.8. Mössbauer spectrum of the sample in Figure 5 following 48 hours in syngas.

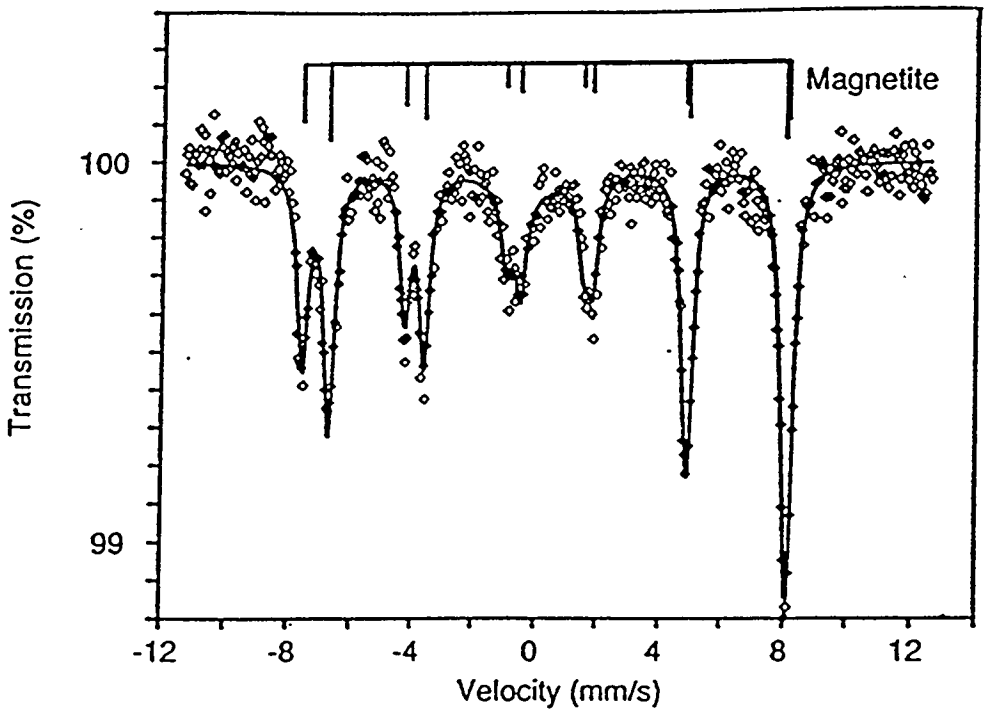

Figure VI.2.9. Mössbauer spectrum of the sample in Figure 5 after 100 hours exposure to synthesis gas.

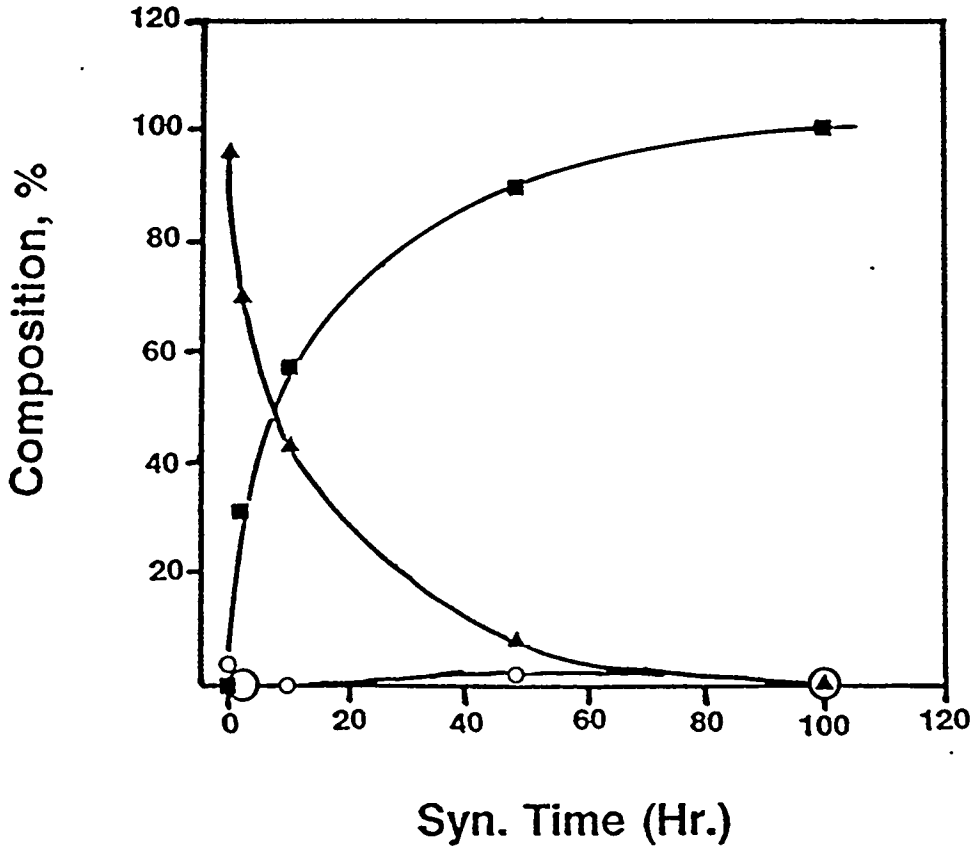

Figure VI.2.10. The change with exposure time in synthesis gas of the iron chemical state following 24 hours of pretreatment in CO (Fe_3O_4, ■, Fe_2O_3, ○; Fe carbides, ▲).

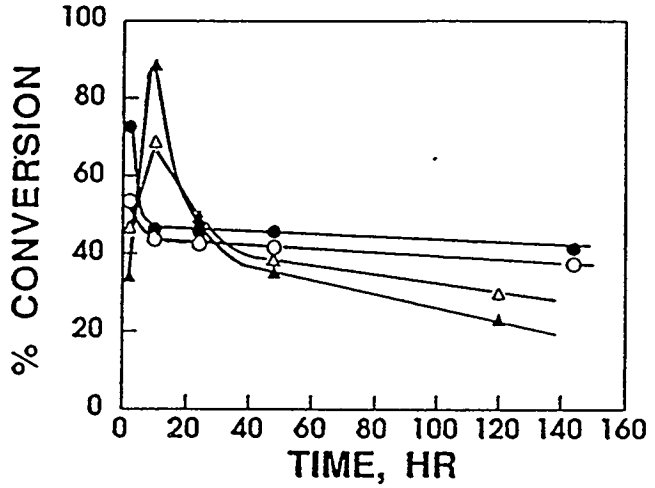

Figure VI.2.11. The dependence of the catalytic activity for CO and H_2 conversion upon the pretreatment [CO conversion for H_2 pretreatment, ●; CO conversion for CO pretreatment, ▲; H_2 conversion for H_2 pretreatment, ○; CO conversion for H_2 pretreatment, △].

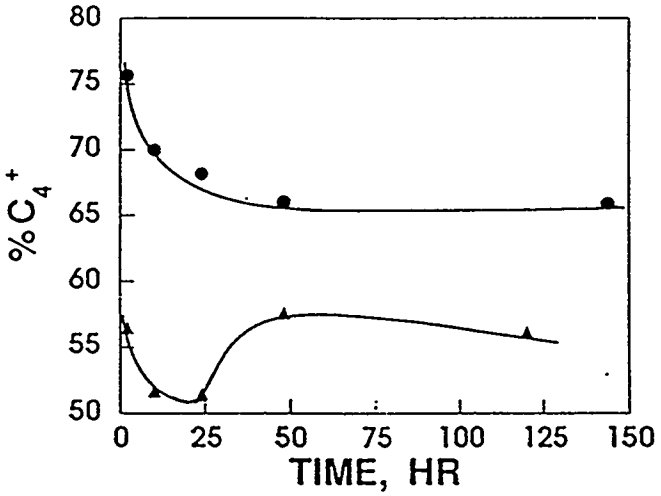

Figure VI.2.12. The fraction of C_4^+ products for the CO pretreated (▲) and the hydrogen pretreated (●) catalysts.